Comparison of Cardiac Sympathetic Nervous Function with Left Ventricular Function and Perfusion in Cardiomyopathies by ^{123}I-MIBG SPECT and ^{99m}Tc-Tetrofosmin Electrocardiographically Gated SPECT

Chunlei Zhao, Noriyuki Shuke, Wakako Yamamoto, Atsutaka Okizaki, Junichi Sato, Yukio Ishikawa, Takahumi Ohta, Naoyuki Hasebe, Kenjiro Kikuchi, and Tamio Aburano

Department of Radiology and First Department of Internal Medicine, Asahikawa Medical College; and Section of Radiology, Asahikawa Medical College Hospital, Asahikawa, Japan

The objective of this study was to clarify the relationship between cardiac sympathetic nervous function (CSNF) and left ventricular (LV) function and perfusion in hypertrophic cardiomyopathy (HCM) and dilated cardiomyopathy (DCM). **Methods:** Thirty-eight cases (32 males, 6 females; mean age, 56 ± 15 y), consisting of 5 healthy control subjects, 15 patients with DCM, and 18 patients with HCM, were studied with ^{123}I-metaiodobenzylguanidine (MIBG) and ^{99m}Tc-tetrofosmin SPECT. CSNF was evaluated from cardiac uptake and washout of MIBG, whereas LV perfusion and function were evaluated from tetrofosmin uptake and wall thickening on electrocardiographically gated SPECT. As quantitative parameters of global cardiac MIBG uptake and washout, the heart-to-mediastinum ratio (H/M) and percentage washout were calculated from early and delayed planar images. As quantitative regional parameters, the regional uptake and percentage washout of MIBG were calculated from SPECT images dividing the left ventricle into 12 segments. In the tetrofosmin study, the H/M and LV ejection fraction were calculated as the parameters of global LV perfusion and function. As quantitative regional parameters, the regional uptake and wall thickening were also calculated for the 12 myocardial segments using the quantitative gated SPECT software. Multiple linear regression analysis was performed to investigate the correlations between the parameters from the 2 studies. **Results:** In DCM and HCM, multiple linear regression analysis of the regional parameters showed significant correlations between LV function and CSNF ($P < 0.0001$) and between LV perfusion and CSNF ($P < 0.0001$). According to the partial correlation coefficients, washout and early uptake of MIBG were the most significant factors for predicting LV function and LV perfusion, respectively. **Conclusion:** In cardiomyopathies, CSNF was closely related to LV function. The quantitative parameters of MIBG washout could reflect cardiac functional impairment. Early MIBG uptake might be determined by myocardial perfusion in cardiomyopathies.

Key Words: hypertrophic cardiomyopathy; dilated cardiomyopathy; ^{123}I-metaiodobenzylguanidine; ^{99m}Tc-tetrofosmin; gated myocardial SPECT

J Nucl Med 2001; 42:1017–1024

Metaiodobenzylguanidine (MIBG) has similar structure and the same uptake and storage mechanisms as norepinephrine (NE) (*1*). MIBG is stored in presynaptic vesicles and is secreted in response to acetylcholine released from the preganglionic neuron (*2*,*3*). ^{123}I-MIBG was developed for evaluating cardiac sympathetic nervous function (CSNF), and the usefulness of ^{123}I-MIBG imaging has been generally accepted for many diseases, such as heart failure, diabetes, Parkinson's disease, and cardiomyopathy (*4*–*9*). Decreased cardiac MIBG uptake was thought to reflect impaired adrenergic nervous function or denervation in these diseases. The heart-to-mediastinum ratio (H/M) at 3–4 h after injection appears to be a good quantitative index of neuronal MIBG uptake in the clinical situation (*1*), although this index is not sensitive enough to detect the slight reduction of MIBG accumulation (*10*). As for the relationship between MIBG uptake and left ventricular (LV) function, decreased MIBG uptake on delayed images was closely related to LV dysfunction in patients with heart failure (*11*,*12*). In other studies, sympathetic denervation was found to exist with normal LV function at rest (*13*,*14*). Cardiac MIBG washout rate is another index that could represent sympathetic nervous activity related to NE storage ability (*15*). However, the clinical significance of this index has not been fully clarified. Patients with cardiomyopathy had rapid washout of MIBG (*8*,*16*), whereas the results were

Received Nov. 14, 2000; revision accepted Mar. 5, 2001.

For correspondence or reprints contact: Chunlei Zhao, MD, Department of Radiology, Asahikawa Medical College, 2-1 Midorigaoka-Higashi, Asahikawa, Japan, 078-8510.

controversial in the patients with diabetes (*17*,*18*). Considering these reported results, the relationship between CSNF and LV function may differ depending on the type of disease and may not be explained by a common theory. In this study, we investigated the relationship between CSNF evaluated from uptake and washout of MIBG and LV function and myocardial perfusion in the patients with dilated cardiomyopathy (DCM) and hypertrophic cardiomyopathy (HCM) to clarify the clinical significance of MIBG imaging in these diseases.

Electrocardiographically (ECG) gated SPECT with ^{99m}Tc-tetrofosmin and the quantitative gated SPECT software were applied to analyze LV perfusion and function simultaneously. This approach could make it easy to compare regional MIBG uptake or washout with LV perfusion or function on a myocardial segment-by-segment basis.

MATERIALS AND METHODS

Thirty-eight cases (32 males, 6 females; mean age, 56 ± 15 y; age range, 15–77 y), consisting of 5 healthy control subjects (normal controls [NCs]), 15 patients with DCM, and 18 patients with HCM, were studied. Seven patients with DCM were clinically diagnosed as having chronic heart failure, and 4 patients with HCM were in the dilated phase. ^{123}I-MIBG SPECT and ^{99m}Tc-tetrofosmin gated SPECT were performed on these subjects within 2 wk without any medical intervention. ^{123}I-MIBG (MyoMIBG-I-123; 111 MBq/0.03–0.10 mg) and the ^{99m}Tc generator system (Ultra-TechneKow) were purchased from Daiichi Radioisotope Laboratory (Tokyo, Japan). ^{99m}Tc-tetrofosmin was prepared using a kit vial of tetrofosmin (Myoview; Nihon-Mediphysics, Tokyo, Japan) and freshly eluted ^{99m}Tc-pertechnetate.

Imaging Protocol

We performed early and delayed ^{123}I-MIBG imaging using a single-head, rotating gamma camera equipped with a low-energy, general-purpose collimator (RC-135E; Hitachimedico, Tokyo, Japan). Early imaging began 15 min after an intravenous injection of 111 MBq ^{123}I-MIBG. Before SPECT acquisition, an anterior chest image was acquired for 300 s in a 128 × 128 matrix. Immediately after planar imaging, 32 images were obtained in a 64 × 64 matrix for 40 s, with a 180° rotation and an energy window of 10% centered at 160 keV. Delayed planar imaging and SPECT imaging were performed 4 h after the injection under the same acquisition conditions as used in the early imaging.

For ECG gated ^{99m}Tc-tetrofosmin SPECT, we used a triple-head, rotating gamma camera equipped with a low-energy, high-resolution collimator (GCA-9300A/DI; Toshiba Medical, Tokyo, Japan). Sixty images were obtained using the R wave on electrocardiography as a trigger of acquisition in a 64 × 64 matrix for 30 s, over 360°, with an energy window of 10% centered at 140 keV at 2 h after an intravenous injection of 740 MBq ^{99m}Tc-tetrofosmin. Each image was partitioned into 8 or 16 frames per cardiac cycle.

Reconstruction was performed without attenuation and scatter correction by a filtered backprojection algorithm for ^{123}I-MIBG and ^{99m}Tc-tetrofosmin studies. After preprocessing with a Butterworth filter (cutoff frequency, 0.44 cycle/cm; power factor, 8), transaxial images were reconstructed with a ramp filter. Long- and short-axial slices were then produced by axial reorientation.

Data Processing

On the anterior planar ^{123}I-MIBG images, regions of interest (ROIs) were drawn over the whole heart and upper mediastinum. Using the counts in the ROIs, the H/M and global cardiac washout (GW) of MIBG were calculated as follows:

$$\text{H/M} = \frac{\text{mean pixel counts of heart ROI}}{\text{mean pixel counts of mediastinum ROI}},$$

$$\text{GW (\%)} = \frac{\text{mean heart pixel counts (early)} - \text{mean heart pixel counts (delayed)}}{\text{mean heart pixel counts (early)}} \times 100,$$

where the H/M from early and delayed images is H/Me and H/Md, respectively. Decay correction was done for calculating GW.

Regional uptake and washout of ^{123}I-MIBG were analyzed using dedicated software after repositioning the center of early and delayed short-axial slices to the same position. In this analysis, the left ventricle was divided into 3 parts from the apex to the base, perpendicularly to the long axis of the heart. Each part was then divided into 6 segments on a short-axial plane: inferior septal, anterior septal, anterior, anterior lateral, inferior lateral, and inferior segments. Twelve segments from middle and apical parts were used (Fig. 1). After drawing circular ROIs on a short-axial plane for determining outer and inner edges of the myocardium, mean voxel counts of each segment were calculated. Using the mean voxel counts, the regional washout (RW) and uptake index (MUP) were calculated on a myocardial-segment basis as follows:

$$\text{RW (\%)} = \frac{\text{mean early segmental counts} - \text{mean delayed segmental counts}}{\text{mean early segmental counts}} \times 100,$$

$$\text{MUP} = \frac{\text{mean segmental counts}}{\text{highest voxel counts in myocardial ROIs}} \times \text{H/M},$$

where the MUP, the product of relative regional uptake and H/M, was introduced to compare absolute regional MIBG uptake. The MUP of early and delayed images is MUPe and MUPd, respectively. Decay correction was done for calculating RW.

To calculate the H/M of ^{99m}Tc-tetrofosmin (H/M-tetrofosmin), ROIs of the heart and mediastinum were drawn on an anterior image from merged nongated SPECT images because planar imaging was not performed in the ^{99m}Tc-tetrofosmin study. Applying the

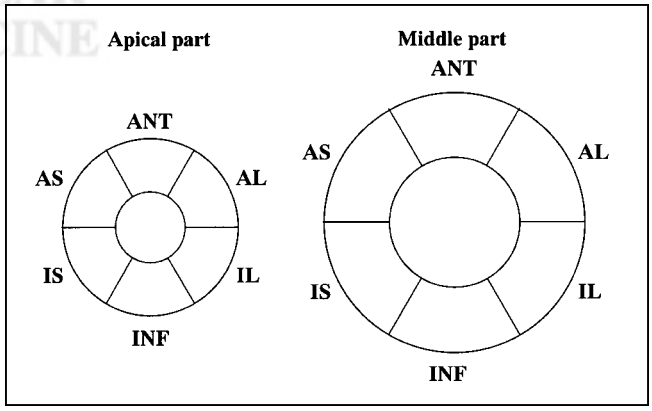

FIGURE 1. Diagram of myocardial segments of left ventricle on short-axial plane. IS = inferior septal; AS = anterior septal; ANT = anterior; AL = anterior lateral; IL = inferior lateral; INF = inferior.

quantitative gated SPECT software to the ECG gated SPECT images, LV ejection fraction (LVEF), wall thickening (TH), and relative regional end-systolic and end-diastolic uptake that was normalized by the highest voxel counts were computed and displayed in the bull's eye maps. The same segments as shown in Figure 1 were used for the analysis. Regional end-systolic uptake was selected as the parameter of regional perfusion. To compare the absolute levels of regional ^{99m}Tc-tetrofosmin uptakes among individual segments, we introduced the uptake index (UPes), defined as the product of regional uptake at end-systole and H/M-tetrofosmin:

$$\text{UPes} = \text{regional uptake at end-systole} \times \text{H/M-tetrofosmin}.$$

The parameters from both studies are summarized in Table 1. Examples of the images of ^{123}I-MIBG and ^{99m}Tc-tetrofosmin studies for NC, DCM, and HCM are shown in Figure 2.

The mean and SD of the TH value calculated from 60 myocardial segments of 5 NCs were used to classify all segments of the patients according to the degree of asynergy. Altogether, 396 segments were divided into 3 groups according to their TH values: normal (N; TH $>$ mean minus SD), moderate asynergic (M; mean minus 2SD $<$ TH $\leq$ mean minus SD), and severe asynergic (S; TH $\leq$ mean minus 2SD). The group means of other regional parameters were calculated and compared on the basis of this classification.

Statistical Analysis

One-way ANOVA was applied for comparing the parameters from ^{123}I-MIBG and ^{99m}Tc-tetrofosmin studies. To determine if the factors were independently related to LV function or perfusion, the parameters from the MIBG study were examined by multiple linear regression analysis. Sample correlation coefficients and partial correlation coefficients were calculated. $P < 0.05$ was considered significant in all tests.

RESULTS

Global Parameters

The means of patients' age and global parameters in NC, DCM, and HCM are listed in Table 2. No significant difference was found in age. The means of LVEF, H/Md, and GW were significantly different among the 3 categories, in decreasing order of NC, HCM, and DCM for LVEF and H/Md and in opposite order for GW. The H/M-tetrofosmin in HCM was significantly greater than that in DCM, but the H/M-tetrofosmin in NC showed no significant differences from those in HCM and DCM. The H/Me in NC and HCM were significantly greater than that in DCM, but no significant difference was found between NC and HCM. Within the DCM category, the LVEF of patients with heart failure showed a significantly lower value than that of patients without heart failure. Within the HCM category, the LVEF and H/Me of patients in nondilated phase were significantly greater than those of patients in dilated phase.

TABLE 1
Global and Regional Parameters in Study

Parameters of CSNF
Global
GW: global % washout of MIBG
H/Me, H/Md: early and delayed H/M in MIBG study
Regional
RW: regional % washout of MIBG
MUPe, MUPd: early and delayed MIBG uptake
Parameters of LV function
Global
LVEF: LV ejection fraction
Regional
TH: wall thickening
Parameters of myocardial perfusion
Global
H/M-tetrofosmin: H/M in tetrofosmin study
Regional
UPes: tetrofosmin uptake at end-systole

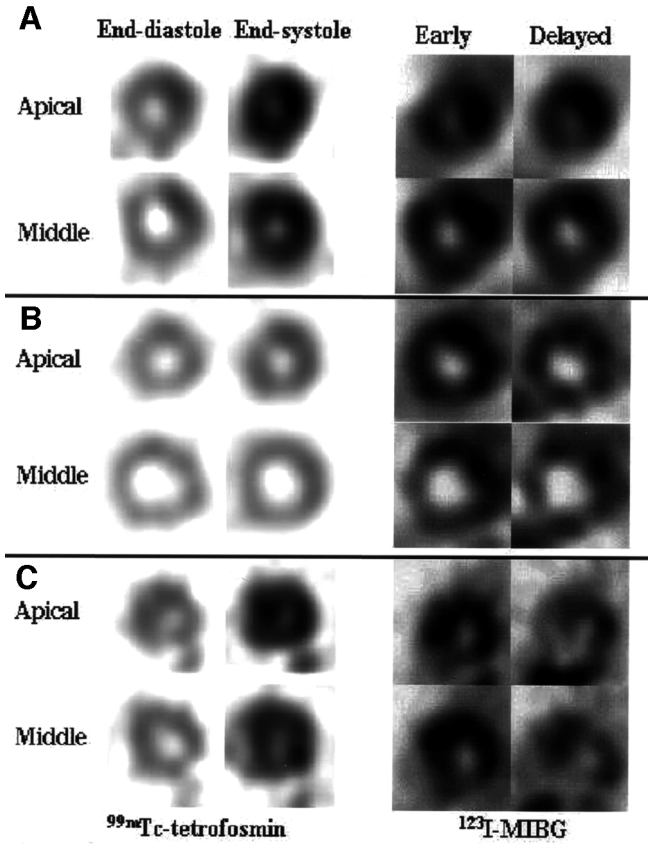

FIGURE 2. Examples of ^{99m}Tc-tetrofosmin and ^{131}I-MIBG SPECT. Short-axial images of 55-y-old healthy man (A), 59-y-old man with DCM (B), and 15-y-old boy with HCM (C). In DCM and HCM, myocardial MIBG uptake was significantly decreased on delayed images.

Regional Parameters

Two patients (1 with DCM and 1 with HCM) were omitted from regional analyses in the MIBG study because of nonvisualization of their hearts.

Descriptive statistics of regional parameters in NC, DCM, and HCM are listed in Table 3. The means of TH, RW, and MUPd among the 3 categories were significantly different, in decreasing order of NC, HCM, and DCM for TH and MUPd and in opposite order for RW. The means of UPes and MUPe were also significantly different among the 3

TABLE 2
Patients' Age and Global Parameters in NC, DCM, and HCM

Parameter	NC (n = 5)	DCM Non-HF (n = 8)	DCM HF (n = 7)	DCM Overall (n = 15)	HCM Non-DP (n = 14)	HCM DP (n = 4)	HCM Overall (n = 18)
Age (y)	47.6 ± 12.68	58.38 ± 15.45	58.14 ± 9.6	58.27 ± 12.6	55.93 ± 19.08	60.25 ± 6.80	56.89 ± 17.03
LVEF (%)	71 ± 11.22	33.5 ± 7.84*	22 ± 8.35*†	28.13 ± 9.79*	50.29 ± 10.82*	37.75 ± 1.5*‡	47.5 ± 10.9*§
H/M-TF	2.92 ± 0.54	2.62 ± 0.31	2.46 ± 0.46	2.55 ± 0.38	3.32 ± 0.51	2.92 ± 0.33	3.23 ± 0.5§
H/Me	2.17 ± 0.05	1.89 ± 0.34	1.8 ± 0.18*	1.85 ± 0.27*	2.39 ± 0.33*	1.91 ± 0.20‡	2.28 ± 0.36§
H/Md	2.66 ± 0.21	1.91 ± 0.48*	1.73 ± 0.39*	1.82 ± 0.44*	2.36 ± 0.29	2.03 ± 0.29*	2.28 ± 0.31*§
GW (%)	11.88 ± 7.23	33.34 ± 9.02*	31.58 ± 11.18*	32.52 ± 9.75*	26.47 ± 7.01*	23.64 ± 10.34	25.84 ± 7.61*§

*$P < 0.05$ vs. NC.
†$P < 0.05$ vs. non-HF.
‡$P < 0.05$ vs. non-DP.
§$P < 0.05$ vs. DCM (overall).
n = case number; Non-HF = nonheart failure; HF = heart failure; Non-DP = nondilated phase; DP = dilated phase; H/M-TF = H/M in tetrofosmin study; H/Me = early H/M in MIBG study; H/Md = delayed H/M in MIBG study.
Data are presented as mean ± SD.

categories, becoming smaller in the order of HCM, NC, and DCM. Within the DCM category, all parameters except UPes showed significant differences between the patients with heart failure and those without heart failure. Within the HCM category, all parameters except RW showed significant differences between the patients in dilated phase and those in nondilated phase. UPes and MUPe of the patients with HCM in dilated phase were significantly decreased compared with NC.

The normal TH value was 54.6% ± 17.7% (mean ± SD). All 396 segments of the patients were classified into N, M, and S groups according to the deviation of their TH values from the normal mean. The group means of RW, UPes, MUPe, and MUPd were significantly different among the 3 groups ($P < 0.05$), and their values were correlated with the degree of asynergy (Fig. 3).

Correlation Among Global Parameters

The values of multiple correlation coefficients between observed values of LVEF and the values predicted from the global MIBG parameters (H/Me, H/Md, and GW) were 0.513 ($P = 0.321$) in DCM and 0.425 ($P = 0.410$) in HCM. These values indicated no significant correlations between LVEF and the global MIBG parameters in DCM and HCM.

The values of multiple correlation coefficients between observed values of H/M-tetrofosmin and the values predicted from the global MIBG parameters were 0.570 ($P = 0.212$) in DCM and 0.774 ($P = 0.0043$) in HCM. Thus, the global MIBG parameters showed only a significant correlation with H/M-tetrofosmin in HCM. The partial correlation coefficients between H/Me, H/Md, GW, and H/M-tetrofosmin were 0.764 ($P < 0.001$), −0.612 ($P < 0.05$), and −0.365 ($P > 0.1$). These values indicated significant correlations of early and delayed MIBG uptake with LV perfusion in HCM.

Correlation Among Regional Parameters

The values of multiple correlation coefficients between observed values of TH and the values predicted from the regional MIBG parameters (MUPe, MUPd, and RW) were 0.535 ($P < 0.0001$) in DCM and 0.407 ($P < 0.0001$) in HCM. These values indicated significant correlations between the regional LV function and the regional MIBG parameters in DCM and HCM. In DCM, the values of partial correlation coefficients between MUPe, MUPd, RW, and TH were 0.280 ($P < 0.001$), −0.123 ($P > 0.1$), and −0.304 ($P < 0.0001$). In HCM, these values were −0.012 ($P > 0.1$), 0.104 ($P > 0.1$), and −0.154 ($P < 0.05$).

The values of multiple correlation coefficients between observed values of UPes and the values predicted from the regional MIBG parameters (MUPe, MUPd, and RW) were 0.560 ($P < 0.0001$) in DCM and 0.552 ($P < 0.0001$) in HCM. These values indicated significant correlations between the regional LV perfusion and the regional MIBG parameters in DCM and HCM. In DCM, the values of partial correlation coefficients between MUPe, MUPd, RW, and UPes were 0.356 ($P < 0.00001$), −0.176 ($P < 0.05$), and −0.328 ($P < 0.0001$). In HCM, these values were 0.307 ($P < 0.00001$), −0.097 ($P > 0.1$), and 0.144 ($P < 0.05$). In DCM and HCM, early MIBG uptake showed the best correlation with LV perfusion.

Table 4 shows sample correlation coefficients between the parameters in DCM and HCM. TH and UPes showed a significant correlation with all regional MIBG parameters. The correlation coefficients between TH and RW were −0.412 ($P < 0.001$) in DCM and −0.350 ($P < 0.001$) in HCM (Fig. 4). The correlation coefficients between UPes and MUPe were 0.419 ($P < 0.001$) in DCM and 0.461 ($P < 0.001$) in HCM (Fig. 5).

DISCUSSION

Cardiomyopathies are myocardial diseases that are often presented with severe cardiac dysfunction and can be classified into dilated, restrictive, and hypertrophic types on the

TABLE 3
Regional Parameters in NC, DCM, and HCM

Parameter	NC	DCM			HCM		
		Non-HF	HF	Overall	Non-DP	DP	Overall
TH (%)	54.55 ± 17.67 (60)	23.51 ± 10.79* (96)	16.82 ± 9.64*† (84)	20.39 ± 10.77* (180)	31.61 ± 14.82* (168)	17.56 ± 5.90*‡ (48)	28.49 ± 14.57*§ (216)
UPes	2.36 ± 0.52 (60)	1.86 ± 0.52* (96)	1.78 ± 0.57* (84)	1.82 ± 0.54* (180)	2.75 ± 0.55* (168)	1.84 ± 0.76*‡ (48)	2.55 ± 0.71*§ (216)
RW (%)	1.04 ± 16.8 (60)	32.08 ± 20.20* (84)	38.18 ± 18.52*† (84)	35.13 ± 19.56* (168)	31.00 ± 14.62* (168)	26.51 ± 18.30*‡ (36)	30.21 ± 15.38*§ (204)
MUPe	1.68 ± 0.29 (60)	1.49 ± 0.40* (84)	1.36 ± 0.33*† (84)	1.43 ± 0.37* (168)	1.90 ± 0.43* (168)	1.30 ± 0.42*‡ (36)	1.79 ± 0.48*§ (204)
MUPd	2.12 ± 0.36 (60)	1.51 ± 0.47* (84)	1.23 ± 0.52*† (84)	1.37 ± 0.51* (168)	1.80 ± 0.49* (168)	1.39 ± 0.55*‡ (36)	1.73 ± 0.52*§ (204)

*$P < 0.05$ vs. NC.
†$P < 0.05$ vs. non-HF.
‡$P < 0.05$ vs. non-DP.
§$P < 0.05$ vs. DCM (overall).
Non-HF = nonheart failure; HF = heart failure; Non-DP = nondilated phase; DP = dilated phase; UPes = tetrofosmin uptake at end-systole; RW = regional % washout of MIBG; MUPe = early MIBG uptake; MUPd = delayed MIBG uptake.
Data are presented as mean ± SD. Values in parentheses are number of myocardial segments.

basis of etiology, pathophysiology, and clinical manifestation (*19*). Cardiac MIBG uptake often decreases in patients with cardiomyopathies; this decrease could reflect abnormal CSNF associated with cardiomyopathy (*8,9,16,20,21*). However, little is known about the relationship between cardiac sympathetic disorders and the pathophysiology of cardiomyopathies, especially LV function and perfusion. In this context, we performed our study and found that CSNF evaluated from cardiac MIBG imaging was closely related to LV function in patients with DCM and HCM.

In this study, the HCMs of the nondilated phase were better compared with NCs in terms of myocardial tetrofosmin uptake and early cardiac MIBG uptake but, on the contrary, were worse in LV function, delayed uptake, and washout of MIBG. These results indicated that LV function and CSNF could be disordered, even though myocardial perfusion was reserved in the HCMs of the nondilated phase. However, among the 3 categories of NC, HCM, and DCM, DCMs had the lowest LV function and perfusion associated with the lowest uptake and the fastest washout of MIBG. These findings were in good agreement with the pathophysiologic characteristics of DCM (*19*).

Previous studies suggested that cardiac MIBG uptake was correlated with the parameters of LV function, such as LVEF, cardiac index, end-diastolic pressure, and regional wall motion, in heart failure (*11*) and myocardial infarction (*1*). However, in cardiomyopathy, the relationship between cardiac MIBG uptake and LV function has not been fully clarified. Cardiac MIBG washout, which is a commonly used parameter in MIBG studies, showed variability in various diseases (*8,16–18*). Yamakado et al. (*20*) reported a significant correlation between cardiac MIBG washout and LV function in DCM. In agreement with this finding, our results showed that regional MIBG washout was the most significant independent factor related to regional function in DCM and HCM. These results suggested that MIBG washout was closely correlated with LV function and could be a useful parameter reflecting LV function in patients with cardiomyopathies. On the basis of the results showing that abnormalities of CSNF were related to impaired LV function in DCM and HCM, the association between CSNF and LV function might be independent of the type of cardiomyopathies.

Earlier studies on patients with DCM and HCM indicated that delayed cardiac MIBG uptake was independent of myocardial blood flow and that MIBG distributed more heterogeneously compared with blood flow tracers in delayed phase (*8,20,21*). However, early cardiac distribution of MIBG was similar to that of blood flow tracers (*20,21*). In keeping with these findings, our results showed that regional early MIBG uptake was the most significant factor for predicting LV function in DCM and HCM. Considering these findings, early MIBG uptake might be largely dependent on the blood flow in DCM and HCM. Simple linear regression analysis showed that regional MIBG washout was inversely correlated with regional perfusion in DCM,

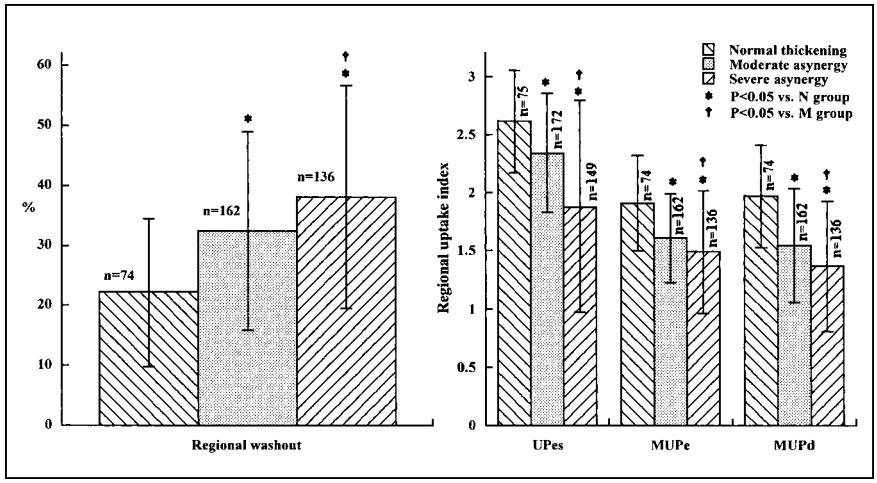

FIGURE 3. Group means of regional parameters. *n* = number of myocardial segments; UPes = tetrofosmin uptake at end-systole; MUPe = early MIBG uptake; MUPd = delayed MIBG uptake.

whereas it was positively correlated with regional perfusion in HCM. These findings imply that the kinetics of MIBG might be different in these 2 types of cardiomyopathies.

Histologic abnormalities of the myocardium in cardiomyopathies (such as degeneration, fibrosis, and so forth) have been reported to be associated with decreased cardiac MIBG uptake (*7*,*9*). These histologic abnormalities in cardiomyopathies might impair sympathetic nervous function or the ability of NE storage, resulting in the reduced uptake and rapid washout of MIBG on delayed images. On the other hand, other studies have indicated that decreased MIBG uptake was related to sympathetic denervation or the impairment of neuronal uptake function in the patients with heart failure and diabetes (*12*,*22*). However, it is unclear in cardiomyopathies whether sympathetic denervation or the impairment of neuronal uptake function causes the decrease of MIBG uptake. We found that, although delayed MIBG uptake decreased in DCM and HCM, early MIBG uptake in the HCMs of the nondilated phase was even better than that in NCs. These findings indicate that the early MIBG uptake mechanism was not damaged in the early phase of HCM. Dae et al. (*23*) found that specific neuronal uptake is dominant in the mechanism of human myocardial NE uptake. Therefore, considering this finding and our results indicating that early MIBG uptake in the HCMs of the nondilated phase was not reduced and early MIBG uptake in HCM was correlated significantly with blood flow, the impairment of neuronal uptake function might not be dominant in HCM. On the other hand, in DCM, early MIBG uptake was worse than that in NCs. However, it is doubtful whether this low early MIBG uptake in DCM is caused by the low perfusion other than the impaired neuronal uptake function, even though our results showed that the low early MIBG uptake was closely associated with the low perfusion in DCM. The mechanisms of the uptake and rapid washout of MIBG in cardiomyopathies remain to be clarified.

The H/M used for normalizing tracer uptake in the study was measured from planar images because it was a simple and reproducible way to evaluate the tracer uptake (*12*).

TABLE 4
Correlation Coefficients (*r* values) Between Regional Parameters

	TH		UPes	
Parameter	DCM (*n* = 168)	HCM (*n* = 204)	DCM (*n* = 168)	HCM (*n* = 204)
RW	−0.412*	−0.350*	−0.372*	0.274*
MUPe	0.356*	0.198*	0.419*	0.461*
MUPd	0.459*	0.349*	0.457*	0.217*

*$P < 0.01$.

UPes = tetrofosmin uptake at end-systole; *n* = number of myocardial segments; RW = regional % washout of MIBG; MUPe = early MIBG uptake; MUPd = delayed MIBG uptake.

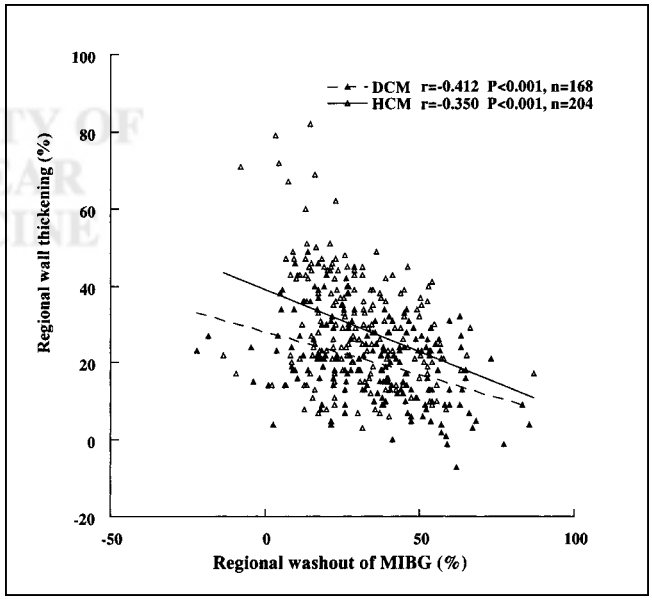

FIGURE 4. Correlation between regional MIBG washout and wall thickening in DCM and HCM. *n* = number of myocardial segments.

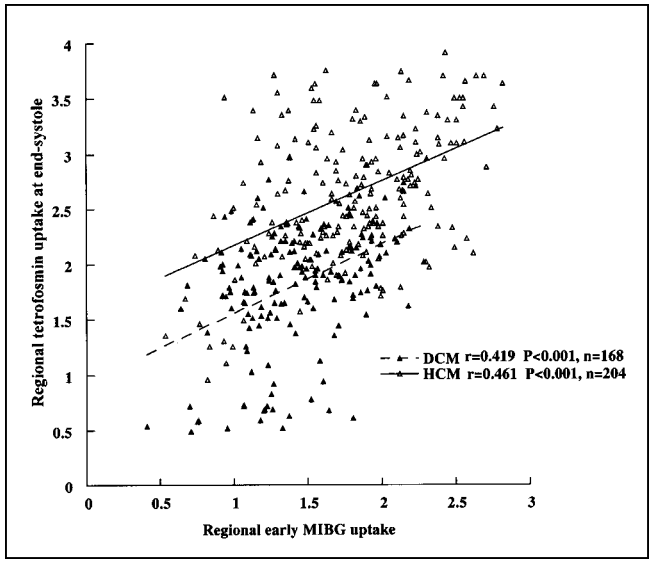

FIGURE 5. Correlation between regional early MIBG uptakes and perfusion in DCM and HCM. *n* = number of myocardial segments.

However, planar imaging had its own limitations because the heart counts included the counts of overlying lung (*12*,*22*). Thus, in the patient whose cardiac uptake of the tracer was decreased significantly, the H/M might be overestimated. We failed to determine the significant global MIBG parameters for predicting LV perfusion in DCM and for predicting LV function in DCM and HCM. This failure might be associated with the small sample; on the other hand, it could be explained by the limitations of the global parameters. A more accurate index should be sought to diminish this error.

Because data from the MIBG and tetrofosmin studies were acquired separately with different machines, the exact matching of the corresponding slices was nearly impossible. However, because the counts in neighboring slices from the same part were not too different (as found in this study), the errors caused by the slice selection might be limited to an acceptable range. We excluded the basal part of the myocardium from the regional analysis because it was relatively difficult to determine the border of this part and the slice selection in this part tended to cause more errors in the quantitative analyses.

The relationship between CSNF and LV function in DCM and HCM was determined in this study. These results suggested that MIBG could be helpful in obtaining pathophysiologic information on the patients with cardiomyopathies. However, it should be noted that the relationship between CSNF and LV function might be more complicated in other diseases. For example, normal cardiac function could coexist with sympathetic denervation in transplanted hearts (*24*). The relationship between MIBG imaging and LV function may vary in different diseases. More studies must be done to further understand the significance of MIBG imaging in different cardiovascular diseases.

CONCLUSION

In patients with DCM and HCM, CSNF was closely related to LV function, the quantitative parameters of MIBG washout that could reflect cardiac functional impairment in cardiomyopathies. Early cardiac MIBG uptake might be largely dependent on the myocardial perfusion in cardiomyopathies.

REFERENCES

1. Valette H, Syrota A. Nuclear techniques in the assessment of myocardial innervation. In: Murry IPC, Ell PJ, eds. *Nuclear Medicine in Clinical Diagnosis and Treatment*. Edinburgh, U.K.: Churchill Livingstone; 1998:1525–1529.
2. Wieland DM, Brown LE, Tobes MC, et al. Imaging the primate adrenal medullae with [^{123}I] and [^{131}I] meta-iodobenzylguanidine. *J Nucl Med*. 1981; 22:358–364.
3. Jaques S Jr, Toes MC. Comparison of the secretory mechanisms of meta-iodobenzylguanidine (MIBG) and norepinephrine (NE) from cultured bovine adrenomedullary cells. *J Nucl Med*. 1985;26:17–26.
4. Atsumi H, Takeishi Y, Fujiwara S, Tomoike H. Cardiac sympathetic nervous disintegrity is related to exercise intolerance in patients with chronic heart failure. *Nucl Med Commun*. 1998;19:451–456.
5. Murata K, Sumida Y, Murashima S, et al. A novel method for the assessment of autonomic neuropathy in type 2 diabetic patients: a comparative evaluation of ^{123}I-MIBG myocardial scintigraphy and power spectral analysis of heart rate variability. *Diabet Med*. 1996;13:266–272.
6. Iwasa K, Nakajima K, Yoshikawa H, Tada A, Taki J, Takamori M. Decreased myocardial ^{123}I-MIBG uptake in Parkinson's disease. *Acta Neurol Scand*. 1998; 97:303–306.
7. Ueda T, Kusachi S, Yamaji H, Morishita N, Mima T, Imai M. Recovery of iodine-123 metaiodobenzylguanidine uptake associated with left ventricular functional recovery in a patient with dilated cardiomyopathy: endomyocardial histological findings before and after the improvement of uptake. *Jpn Heart J*. 1997;38:145–150.
8. Yoshimura N, Kimura M, Ozaki T, Takahashi N, Sakai K. Two patients with hypertrophic cardiomyopathy showing regionally increased washout of ^{123}I-MIBG from the thick myocardium [in Japanese]. *Kaku Igaku*. 1998;35:315–320.
9. Murata K, Kusachi S, Murakami T, et al. Relation of iodine-123 metaiodobenzylguanidine myocardial scintigraphy to endomyocardial biopsy findings in patients with dilated cardiomyopathy. *Clin Cardiol*. 1997;20:61–66.
10. Hattori N, Tamaki N, Hayashi T, et al. Regional abnormality of iodine-123-MIBG in diabetic hearts. *J Nucl Med*. 1996;37:1985–1990.
11. Schofer J, Spielmann R, Schubert A, Weber K, Schluter M. Iodine-123 metaiodobenzylguanidine scintigraphy: a noninvasive method to demonstrate myocardial adrenergic system disintegrity in patients with idiopathic dilated cardiomyopathy. *J Am Coll Cardiol*. 1988;12:1252–1258.
12. Merlet P, Valette H, Dubois-Rande JL, et al. Prognostic value of cardiac metaiodobenzylguanidine imaging in patients with heart failure. *J Nucl Med*. 1992; 33:471–477.
13. Langer A, Freeman MR, Josse RG, Armstrong PW. Metaiodobenzylguanidine imaging in diabetes mellitus: assessment of cardiac sympathetic denervation and its relation to autonomic dysfunction and silent myocardial ischemia. *J Am Coll Cardiol*. 1995;25:610–618.
14. Wakasugi S, Fishchman AJ, Babich JW, et al. Metaiodobenzylguanidine: evaluation of its potential as a tracer for monitoring doxorubicin cardiomyopathy. *J Nucl Med*. 1993;34:1283–1286.
15. Nagamachi S, Jinnouchi S, Kurose T, et al. ^{123}I-MIBG myocardial scintigraphy in diabetic patients: relationship with ^{201}Tl uptake and cardiac autonomic function. *Ann Nucl Med*. 1998;12:323–331.
16. Henderson EB, Kahn JK, Corbett JR, et al. Abnormal I-123 myocardial metaiodobenzylguanidine washout and distribution may reflect myocardial adrenergic derangement in patients with congestive heart cardiomyopathy. *Circulation*. 1988;78:1192–1199.
17. Nagamachi S, Jinnouchi S, Nakahara H, et al. ^{123}I-MIBG myocardial scintigraphy in diabetic patients: relationship to autonomic neuropathy. *Nucl Med Commun*. 1996;17:621–632.
18. Mantysaari M, Kuikka J, Mustonen J, et al. Noninvasive detection of cardiac

sympathetic nervous dysfunction in diabetic patients using [123I]metaiodobenzylguanidine. *Diabetes*. 1992;41:1069–1075.
19. Stevenson LW. Diseases of the myocardium. In: Bennett JC, Plum F, eds. *Cecil Textbook of Medicine*. Philadelphia, PA: WB Saunders; 1996:327–336.
20. Yamakado K, Takeda K, Kitano T, et al. Serial change of iodine-123 metaiodobenzylguanidine (MIBG) myocardial concentration in patients with dilated cardiomyopathy. *Eur J Nucl Med*. 1992;19:265–270.
21. Nakajima K, Bunko H, Taki J, Shimizu M, Muramori A, Hisada K. Quantitative analysis of 123I-meta-iodobenzylguanidine (MIBG) uptake in hypertrophic cardiomyopathy. *Am Heart J*. 1990;119:1329–1337.
22. Kim SJ, Lee JD, Ryu YH, et al. Evaluation of cardiac sympathetic neuronal integrity in diabetic patients using iodine-123 metaiodobenzylguanidine. *Eur J Nucl Med*. 1996;23:401–406.
23. Dae MW, De Marco T, Botvinick EH, et al. Scintigraphic assessment of MIBG uptake in globally denervated human and canine hearts: implications for clinical studies. *J Nucl Med*. 1992;33:1444–1450.
24. Bengel F, Schiepel P, Ueberfuhr P, Nekolla S, Reichart B, Schwaiger M. Effect of sympathetic reinnervation on efficiency of the transplanted heart [abstract]. *J Nucl Med*. 2000;41(suppl):50P.